



# Point-by-point femtosecond laser micro-processing of independent core-specific fiber Bragg gratings in a multi-core fiber

A. DONKO,\* M. BERESNA, Y. JUNG, J. HAYES, D. J. RICHARDSON, AND G. BRAMBILLA

Optoelectronics Research Centre, University of Southampton, Southampton, SO17 1BJ, UK

\*a.l.donko@soton.ac.uk

**Abstract:** Four 3rd order fiber Bragg gratings were inscribed into separate cores of a 7 core multi-core fiber using the point-by-point inscription technique. A 1030 nm,  $206 \pm 5$  fs laser was used, operating at a frequency of 1 kHz and pulse energy of  $2.1 \pm 0.2$   $\mu$ J. Independent Bragg resonances at  $\lambda_B = 1541.01 \pm 0.02$ ,  $1547.82 \pm 0.02$ ,  $1532.66 \pm 0.02$ , and  $1537.42 \pm 0.02$  nm and extinction ratios of  $13.97 \pm 0.4$ ,  $16.02 \pm 0.4$ ,  $10.08 \pm 0.4$  and  $13.40 \pm 0.4$  dB were recorded. Our data analysis shows that refractive index changes,  $\Delta n$ , of the order  $10^{-3}$  were induced. Core-specific inscription of fiber Bragg gratings in a multi-core fiber can provide a flexible and versatile platform to address the needs of recent space division multiplexed transmission and optical sensor networks.

Published by The Optical Society under the terms of the [Creative Commons Attribution 4.0 License](#). Further distribution of this work must maintain attribution to the author(s) and the published article's title, journal citation, and DOI.

**OCIS codes:** (060.3735) Fiber Bragg gratings; (060.2340) Fiber optics components

## References and links

1. R. J. Essiambre and R. W. Tkach, "Capacity trends and limits of optical communication networks," *Proc. IEEE* **100**(5), 1035–1055 (2012).
2. H. N. Saha, A. Mandal, and A. Sinha, "Recent Trends in the Internet of Things," in *IEEE 7th Annual Computing and Communication Workshop and Conference* (2017), pp. 1–4.
3. D. J. Richardson, J. M. Fini, and L. E. Nelson, "Space-division multiplexing in optical fibres," *Nat. Photonics* **7**(5), 354–362 (2013).
4. S. Iano, T. Sato, S. Sentsui, T. Kuroha, and Y. Nishimura, "Multicore optical fiber," in *Optical Fibre Communications Conference* (OSA, 1979), pp. 44–46.
5. T. Hayashi, T. Taru, O. Shimakawa, T. Sasaki, and E. Sasaoka, "Design and fabrication of ultra-low crosstalk and low-loss multi-core fiber," *Opt. Express* **19**(17), 16576–16592 (2011).
6. S. Jain, T. Mizuno, Y. Jung, Q. Kang, J. Hayes, M. Petrovich, G. Bai, and H. Ono, "32-core inline multicore fiber amplifier for dense space division multiplexed transmission system," in *The European Conference on Optical Communication* (IEEE, 2016).
7. E. Lindley, S.-S. Min, S. Leon-Saval, N. Cvetojevic, J. Lawrence, S. Ellis, and J. Bland-Hawthorn, "Demonstration of uniform multicore fiber Bragg gratings," *Opt. Express* **22**(25), 31575–31581 (2014).
8. C. G. Askins, T. F. Taunay, G. A. Miller, B. M. Wright, J. R. Peele, L. R. Wasserman, and E. J. Friebele, "Inscription of fiber Bragg gratings in multicore fiber," in *Bragg Gratings, Photosensitivity and Poling in Glass* (OSA, 2007).
9. K. M. Davis, K. Miura, N. Sugimoto, and K. Hirao, "Writing waveguides in glass with a femtosecond laser," *Opt. Lett.* **21**(21), 1729–1731 (1996).
10. D. Grobnc, S. J. Mihailov, C. W. Smelser, and R. T. Ramos, "Ultrafast IR laser writing of strong Bragg gratings through the coating of high Ge-doped optical fibers," *IEEE Photonics Technol. Lett.* **20**(12), 973–975 (2008).
11. G. D. Marshall, R. J. Williams, N. Jovanovic, M. J. Steel, and M. J. Withford, "Point-by-point written fiber-Bragg gratings and their application in complex grating designs," *Opt. Express* **18**(19), 19844–19859 (2010).
12. M. Ams, G. Marshall, D. Spence, and M. Withford, "Slit beam shaping method for femtosecond laser direct-write fabrication of symmetric waveguides in bulk glasses," *Opt. Express* **13**(15), 5676–5681 (2005).
13. A. Donko, Y. Jung, M. Beresna, J. Hayes, D. J. Richardson, and G. Brambilla, "Dataset for Point-by-point Femtosecond Laser Micro-processing of Independent Core-Specific Fiber Bragg Gratings in a Multicore Fiber," <https://eprints.soton.ac.uk/415153/>.
14. R. Feded and M. N. Zervas, "Effects of random phase and amplitude errors in optical fiber Bragg gratings," *J. Lightwave Technol.* **18**(1), 90–101 (2000).

## 1. Introduction

Internet traffic has grown exponentially over the past three decades and shows no indication of slowing [1]. The rapid development of many data centric technological innovations, such as cloud computing and the “Internet of Things”, has created an increasing necessity to improve the efficiency and capacity of data transmission methods [2]. Space division multiplexing (SDM) is frequently portrayed as one of the main contenders for solving this global hurdle. In SDM systems, improved bandwidth is achieved either by increasing the number of cores in an optical fiber, by increasing the number of modes the fiber supports, or by a combination of the two [3]. Each additional mode or core defines a separate information channel, improving the efficiency of data transmission. The concept of SDM can be dated as far back as 1979, but its implementation has been limited by a series of engineering and practicality challenges [4]. Fiber fabricators have since made high capacity, low loss and low cross-talk transmission in multi-core fibers (MCFs) a reality; however, the next challenge in applying SDM solutions lies in producing the necessary associated supporting component and subsystem hardware [5,6].

One of the most basic approaches to SDM requires that each channel multiplexed in the spatial dimension is completely independent of all other channels – most commonly implemented by incorporating multiple cores in the fibre cross-section that are isolated from each other through a combination of core separation and detailed core design. Onward development of this approach requires technological means to independently manipulate the signals propagating in a given core. One of the envisioned key components for such SDM systems is likely to be FBGs for dispersion compensation or filtering purposes. Previously, FBGs have been inscribed in MCFs by simultaneously illuminating all cores of the MCF through a single phase mask [7,8]. This approach can lead to non-uniform exposure across different cores and to effective Bragg grating period discrepancies, which can be difficult to control. Although uniform gratings across all cores have been demonstrated, the flexibility to separately fabricate FBGs of differing period in each core would be a more pragmatic solution in SDM where the cores are independent of one another.

Femtosecond laser assisted inscription could be a viable solution for core-specific multi-core fiber Bragg grating (MC-FBG) fabrication. Femtosecond pulses, exploiting multiphoton absorption and avalanche ionisation, can induce structural modifications in materials otherwise considered non-photosensitive [9]. In addition, by selecting an infrared inscription wavelength, it is not necessary to remove the fiber’s protective coating (polyimide and acrylate are transparent to infrared radiation) [10]. By focussing a femtosecond laser through a high numerical aperture lens, each core can be addressed individually. The point-by-point technique allows not only the writing of each individual grating plane into each core of the MCF, but also provides extra flexibility in grating structure such as chirp or amplitude modulation without significantly modifying the inscription setup [11].

In this paper, we present results on the writing of MC-FBGs suitable for band rejection purposes in SDM applications. Four FBGs were inscribed in four individual cores of a 7 core MCF using the point-by-point technique. Each Bragg grating had a different pitch illustrating the flexibility of the methodology employed.

## 2. Experimental methodology

The MC-FBGs were fabricated using a solid state Yb:KGW (ytterbium-doped potassium gadolinium tungstate) laser (PHAROS, Light Conversion) delivering femtosecond pulses at a central wavelength  $\lambda \sim 1030$  nm, where the fiber’s polymer coating is transparent meaning that it does not need to be removed prior to grating inscription. The laser operated at a repetition rate of 1 kHz with a temporal duration of  $206 \pm 5$  fs and a pulse energy of  $2.1 \pm 0.2$   $\mu$ J.

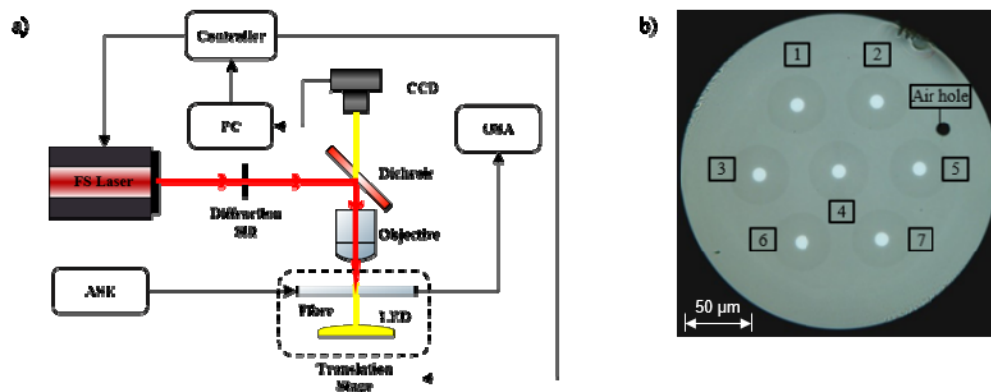


Fig. 1. a) Schematic diagram of the point-by-point femtosecond inscription arrangement. b) Annotated microscope image of the 7 core MCF cross section used for the fabrication of FBGs.

The beam was guided through a diffraction slit prior to being focussed by a 0.65 NA objective lens. Diffraction slits are a common alternative to other beam-shaping optics in femtosecond writing arrangements, employed to control the symmetry of the machined modification [12]. In the absence of beam shaping optics, the modification cross section along the fiber propagation axis is asymmetric – the depth of the modification is minimal as it is dictated by the confocal parameter of the writing beam. By reducing the beam waist in one dimension, the Rayleigh range is decreased causing greater beam divergence, thus increasing the depth of the modification. After the diffraction slit, the inscription beam had a fluence of  $5.25 \pm 0.50 \text{ J/cm}^2$ . The diameter of the beam across the core was observed to be  $6.00 \pm 0.50 \mu\text{m}$ .

A dichroic mirror was positioned directly above the objective lens to allow a CCD camera to provide in situ monitoring of the writing process. The visualisation system allowed positioning of the fiber with respect of laser focal point to a precision of  $\pm 100 \text{ nm}$ . The point-by-point fabrication technique was used; the fiber was traversed beneath the objective at a constant speed producing a uniform grating by individually writing a single plane with a single laser pulse. The grating pitch was governed by a synchronisation controller, which referenced a pulse picker within the laser system to the fiber's position. The shutter frequency differs from the laser frequency as it is dictated by the grating period. Therefore, use of the synchronisation controller causes beating to occur between the laser frequency and the shutter frequency. However, computer simulations showed the effect on the grating pitch to be negligible. Using a fan-in-fan-out device, each core of the MCF was connected to a single mode telecommunication fiber (Corning SMF-28.) This enabled use of an EDFA as a broadband laser source (ASE) and an optical spectrum analyser (OSA, Yokogawa) to provide an in situ measurement of the transmission spectra of each grating. Figure 1(a) displays a schematic of the experimental arrangement.

Before the inscription of the FBG, calibration and optimisation of the inscription beam was completed. Trial pulses were directed into the cladding to ensure the focal point of the laser lay within the image plane of the CCD image. Afterwards, trial pulses were fired into the core to verify the quality of the induced modification.

The MCF was fabricated in-house using the stack-and-draw technique. It consists of seven single mode fiber (SMF) cores arranged in a hexagonal array. Figure 1(b) shows a microscope image of the fiber cross section. All cores are  $10 \mu\text{m}$  in diameter and are surrounded by a cladding  $198 \mu\text{m}$  in diameter. Each core has a numerical aperture of 0.12 and the average core pitch is  $50 \mu\text{m}$ . A continuous air hole is deliberately incorporated in the fiber for orientation purposes.

### 3. Results

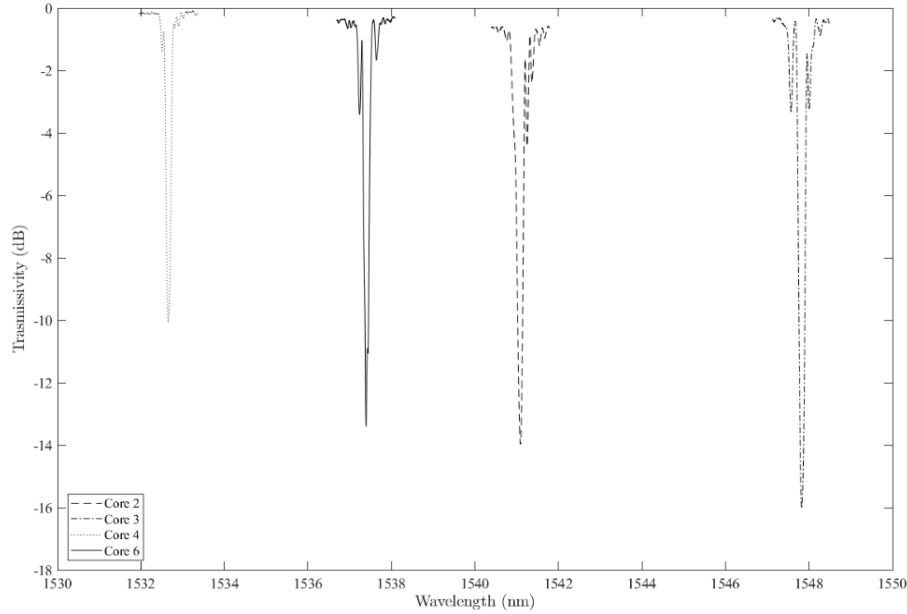


Fig. 2. Transmission spectra of cores 2, 3, 4 and 6 in which the Bragg gratings of resonance wavelengths  $\lambda_B \sim 1541, 1548, 1532$  and  $1538$  nm, had extinction ratios  $\sim 14, 16, 10$  and  $13$  dB respectively.

Computational simulations generated lines of best fit for the data. From coupled mode theory, the reflectivity spectrum of an ideal uniform grating can be described by:

$$r = \frac{\sin^2 \left( \sqrt{\kappa^2 - \hat{\sigma}^2} L \right)}{\cosh^2 \left( \sqrt{\kappa^2 - \hat{\sigma}^2} L \right) - \frac{\hat{\sigma}^2}{\kappa^2}} \quad (1)$$

where  $\kappa$  is the “AC” coupling coefficient, is the general self coupling coefficient and  $L$  is the length of the grating [14]. Using Eq. (1) and inputting the grating period, the resonance wavelength and a trial value of the refractive index modification induced, a line of best fit was applied to the recorded transmission spectra. An iterative algorithm determined the DC refractive index of the FBG by finding the value of minimal variance. Subsequently, the refractive index modulation,  $\Delta n$ , was calculated based upon the 3rd diffraction order of a periodic step index profile.

Four 3rd order FBGs of were inscribed into cores 2, 3, 4 and 6 of the fiber with Bragg resonances  $\lambda_B = 1541.01 \pm 0.02, 1547.82 \pm 0.02, 1532.66 \pm 0.02$ , and  $1537.42 \pm 0.02$  nm and extinction ratios of  $13.97 \pm 0.4, 16.02 \pm 0.4, 10.08 \pm 0.4$  and  $13.40 \pm 0.4$  dB, respectively. No inter-core crosstalk was observed within the 50 dB dynamic range of the measurement. The resultant transmission spectra are displayed in Fig. 2. The transmission spectra data set is available at [13] ([Dataset 1](#)). A CCD image of the grating written in core 3 can be seen in Fig. 3.

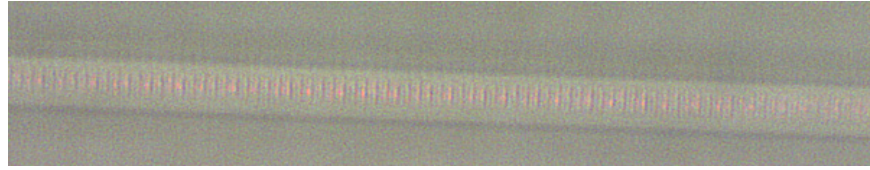


Fig. 3. A CCD image of the core 3 FBG. The image is slanted due to the orientation of the fibre during capture. The grating had a pitch =  $1.605 \pm 0.1 \mu\text{m}$  and refractive index modulation,  $\Delta n = (1.55 \pm 0.03) \times 10^{-4}$ . A red laser diode was connected to core 3 and radiation mode coupling was observed.

Each grating was 8 mm in length and was inscribed in 80 seconds. Measurements of the Bragg resonance wavelength,  $-3$  dB bandwidth, extinction ratio and refractive index modulation are summarised in Table 1. Errors in the period, wavelength and bandwidth arise from the precision of the equipment used.

Table 1. Computational analysis of the FBGs.

Core Number	Period ( $\mu\text{m}$ )	Bragg Wavelength $\lambda_B$ (nm)	$-3\text{dB}$ Bandwidth (nm)	Extinction Ratio (dB)	Refractive index modulation $\Delta n$ ( $\times 10^{-3}$ )
2	$1.598 \pm 0.001$	$1541.01 \pm 0.02$	$0.28 \pm 0.03$	$13.97 \pm 0.40$	$2.56 \pm 0.06$
3	$1.605 \pm 0.001$	$1547.82 \pm 0.02$	$0.22 \pm 0.03$	$16.02 \pm 0.40$	$2.92 \pm 0.06$
4	$1.589 \pm 0.001$	$1532.66 \pm 0.02$	$0.16 \pm 0.03$	$10.08 \pm 0.40$	$2.07 \pm 0.02$
6	$1.594 \pm 0.001$	$1537.42 \pm 0.02$	$0.18 \pm 0.03$	$13.40 \pm 0.40$	$2.38 \pm 0.17$

A 40% difference in the refractive index modulation was observed between the gratings in core 3 and 4, translating into a 7.5% variation in transmission at their respective Bragg resonance wavelengths. It is thought that these variations originate from the  $2 \mu\text{m}$  disparity between the core diameter and the spot diameter in the focal volume. For the fundamental mode, a deviance of  $1 \mu\text{m}$  from the centre of the core can cause a reduction of  $\sim 10\%$  in reflectivity. This is caused by reduced overlap of the induced modification with the power distribution of the fundamental mode. Beam expanding optics can be introduced to increase the size of the beam at the focal point ensuring full overlap between the grating plane and the fundamental mode travelling within the core. In addition, a larger than expected bandwidth was measured for the core 2 FBG. It is believed this is due to the location of core 2 during inscription leading to systematic errors in the grating period. Core 2 was situated furthest from the writing beam and given the fibre orientation during inscription, the beam propagation path was non-uniform. The non-uniformity causes a distortion of the modification symmetry and thus the periodicity, causing a broadening of the bandwidth. The result demonstrates the possibility to access the deepest cores, lying furthest from the surface. However, the quality of the grating can be improved by positioning the core of interest as close to the writing beam as possible. Further refinement of the experimental set up to permit precise rotation of the fibre could accommodate for this.

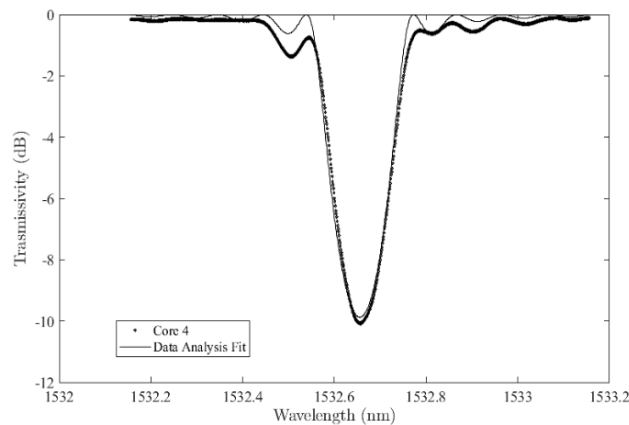


Fig. 4. The transmission spectra of the grating inscribed within core 4 of Bragg resonance  $\lambda_B = 1532.66 \pm 0.02$  nm, extinction ratio =  $10.08 \pm 0.4$  dB and  $-3$ dB bandwidth of  $0.16 \pm 0.02$  nm. Computational analysis applied a line of best fit and deduced the refractive index modulation associated to the grating planes  $\Delta n = (2.07 \pm 0.02) \times 10^{-3}$ .

Figure 4 shows the simulated and measured transmission spectra for core 4. On the short wavelength side of the Bragg resonance, the measured spectrum exhibits a side-lobe suppression ratio half as large as that predicted by simulations. From literature, the increased reflectivity is attributable to random phase errors between the grating planes [14]. The secondary side lobes of the inscribed grating are situated 0.11 nm from the Bragg wavelength and are in agreement with the simulated side lobe location to 3%. The presence of these side lobes verify that a uniform grating was inscribed; apodization would suppress these side lobes and any chirping would show broadening of the Bragg resonance. Side lobes were present in the transmission spectra of all four gratings.

#### 4. Conclusion

In conclusion, using femtosecond laser inscription, FBGs of varying pitch were inscribed into four individual cores of a MCF. Good consistency in the magnitude of the refractive index change was achieved, however, variations of 7.5% in transmission were observed between cores 3 and 4. The inhomogeneity in reflectivity could be mitigated by expanding the spot size cover the area of the core. With further refinement of the experimental set up, it would be possible to access 6 cores; it is not possible to inscribe in core 5 due to the proximity of the air hole distorting the imaging. Theoretically, there is no limit on the number of cores that can be inscribed within a MCF as long as each is clearly accessible – the writing beam should not be obscured by the presence of other cores or air holes. Thus, the point-by-point femtosecond inscription technique has demonstrated its potential for SDM applications. Its precise nature permits manipulation of an individual core within a MCF. Furthermore, using a 1030 nm source the gratings could be inscribed without the removal of the polymer coating. If necessary, the same arrangement would permit fabrication of more complex Bragg grating profiles through further programming of the synchronization controller.

#### Funding

UK Engineering and Physical Sciences Research Council (EPSRC) (EP/L01243X/1, EP/N00762X/1); The Royal Academy of Engineering (RAE) (Ultrafast laser induced nanostructuring: a pathway to advanced optical fibre engineering).